Zwitterionic Poly(carboxybetaine) Brush/Albumin Conjugate Films: Structure and Lubricity

Yuji Higaki, [†*] *Riku Furusawa,* [§] *Takefumi Otsu,* [⊥] *and Norifumi L. Yamada* [#]

[†] Department of Integrated Science and Technology, Faculty of Science and Technology, Oita University, 700 Dannoharu, Oita, 870-1192, Japan

[§] Graduate School of Engineering, Oita University, 700 Dannoharu, Oita, 870-1192, Japan

[⊥] Department of Innovative Engineering, Faculty of Science and Technology, Oita University, 700 Dannoharu, Oita, 870-1192, Japan

[#] Institute of Materials Structure Science, High Energy Accelerator Research Organization, Ibaraki 319-1106, Japan

* Corresponding author

ABSTRACT

Artificial cartilages build up a highly lubricious system with the harmony of biomacromolecules and water. Bioconjugate thin films composed of a zwitterionic poly(carboxybetaine methacrylate) (PCB) brush platform and bovine serum albumin (BSA) were designed. BSA conjugation to the PCB brush chains was achieved by carbodiimide chemistry to give PCB brush/BSA conjugate films. The PCB brush/BSA conjugate films exhibited adaptable interfacial properties due to the amphiphilic nature of BSA. Neutron reflectivity showed that the BSAs are localized at the liquid side of the conjugate films in PBS buffer and the BSA conjugation slightly reduces the water content of the top layer, while the swollen state of the carpet PCB brush layer remained unchanged. The PCB brush/BSA conjugate films showed improved lubricity in the boundary lubrication mode, but slightly worse fluid lubrication induction properties. This conjugate film could be a model system for the investigation of zwitterion/protein composite interfaces and is worth developing biomaterials that require lubrication in vivo.

1. INTRODUCTION

Articular cartilages achieve excellent lubrication performance by employing hybrid molecular systems including collagen, lubricin, proteoglycan, and synovial fluids.[1] The hydrophilic proteoglycan bottle brush chains are grafted on the collagen network to afford affinity with water and macromolecules in the synovial fluids containing proteins and glycosaminoglycans. The highly viscous well-hydrated proteoglycan interfacial layer induces elastohydrodynamic lubrication, where a fluid film is produced during sliding.[2] The liquid infusion and confinement

in the proteoglycan layer at the sliding interface are considered an important aspect of the induction of fluid lubrication.[3] Numerous artificial composite materials that mimic the hierarchical structure of the cartilages have been proposed.[4, 5] As a macromolecular system that mimics the articular cartilages, polymer brushes with hydrophilic polymer chains have been investigated, and the excellent lubricating performance has been demonstrated in a huge number of reports in the past.[6-16] In particular, charged polymer chains including polyelectrolytes and zwitterionic polymers exhibit outstanding lubrication performance in wet conditions. The electrostatic long-range repulsive forces and/or strong hydration are attributed to the enormous lubrication. However, more complex interfacial molecular designs involving multi-component molecules are required for further lubrication performance in physiological conditions.

Zwitterionic polymers have been investigated as an alternative to poly(ethylene oxide), which is the most commonly used bio-passive polymer in the medical field.[17-20] Because of the neutral net charge and affinity with water, the zwitterionic polymers are inert to biomolecules to exhibit anti-blood-clotting and anti-fouling capabilities in physiological conditions. Thus, zwitterionic polymers are the superior platform of biomolecules to maintain the activity and performance without denaturation through undesirable interactions.[21-23] Kaar and co-workers reported a marked improvement in the catalytic activity of lipase, which is an enzyme that catalyzes the hydrolysis of fats, immobilized to zwitterionic poly(sulfobetaine methacrylate) brush by their stabilization.[23]

In this study, we propose a fabrication procedure for composite thin films composed of a zwitterionic poly(carboxybetaine methacrylate) (PCB) brush platform and bovine serum albumin (BSA). BSA is known as a water-soluble protein often applied for passivation, and has been reported to be involved in the lubrication of articular cartilages.[24, 25] Since the PCB chains

contain carboxylate in the carboxybetaine units, amine-containing biomolecules can be introduced through carbodiimide chemistry. We shed light on the wettability and nonuniform structure of the PCB brush/BSA conjugate films in PBS buffer, employing contact angle measurement and neutron reflectivity (NR). Since the conjugation of protein to the zwitterionic polymer brush would bring a positive impact on the lubricating performance, the coefficient of friction was verified by a ball-on-plate reciprocating friction test, and the lubrication mechanism was discussed based on the structure and wettability.

2. EXPERIMENT

2.1 Materials

2-[(*N*-2-methacryloyloxyethyl-*N,N*-dimethyl)ammonio]acetate (CBM) was a kind donation from Osaka Organic Chemical Industry Ltd. (Osaka, Japan), and used without further purification. Copper(I) bromide [Cu(I)Br, FUJIFILM Wako Pure Chemical Corp. (Wako), 99%] was purified by repeating washing with acetic acid followed by ethanol three times then drying under vacuum before use. Tetrahydrofuran (Wako, 97%) was purified by distillation in the presence of calcium hydride. 1-Ethyl-3-(3-dimethylaminopropyl) carbodiimide [EDC, Tokyo Chemical Industry Co., Ltd. (TCI), 98.0%), *N*-hydroxy succinimide (NHS, Wako), and 2-morpholinoethanesulfonic acid, monohydrate (MES, Wako, 99.9%), and Bovine Serum Albumin (BSA, Fraction V, pH7.0, Wako) were used as received. 2-Bromo-2-methyl-propionyloxyhexyltriethoxysilane (BHE) was synthesized following the previous report.[26] Other reagents were purchased from Sigma-Aldrich Co., Wako or TCI, and used as received. Milli-Q water (Millipore Inc., Billerica, MA) with a resistance of >18 MΩ·cm was used for solution

preparation and dialysis. Regenerated cellulose membrane (Spectra/Por 5, MWCO: 12-14 kD) was used as a dialysis bag. Phosphate buffered saline (PBS) was produced by dissolving a tablet (Takara Bio Inc.) into Milli-Q water or D_2O (Kanto Chemical Co., Inc., 99.8%). MES buffer was produced by adjusting the pH of 10 mM MES aqueous solution to 5.0 through the addition of 10 mM NaOH aqueous solution. Custom-made silicon substrates (10 mm × 40 mm × 0.5 mmt for X-ray photoelectron spectroscopy (XPS) and contact angle experiments; 20 mm × 50 mm × 8 mmt for NR) were purchased from Matsuzaki Seisakusyo Co. Ltd. (Shimane, Japan). The silicon substrates were washed before use by repeating the process of sonication in ethanol for 10 minutes followed by exposure to vacuum ultraviolet rays (VUV, λ = 172 nm) under reduced pressure for 10 minutes employing custom-made apparatus (USHIO INC., Tokyo, Japan).

2.2 Measurements

Instruments and conditions for ^{1}H-NMR, gel permeation chromatography (GPC), XPS, and contact angle measurement are described in the SI.

2.2.1 Neutron Reflectivity

NR was conducted using the SOFIA reflectometer [Materials and Life Science Facility (MLF), Japan Proton Accelerator Research Complex (J-PARC), Tokai, Japan].[27, 28] The reflected neutrons were recorded by a two-dimensional position-sensitive scintillation detector. The neutron momentum transfer vector is defined as $q_z = (4\pi \sin\theta)/\lambda$, where θ is the specular reflection angle with respect to the surface. NR for the thin films under the PBS D_2O buffer was acquired by using a homemade liquid cell composed of quartz trough sandwiched with Al plates. The sample was placed in a thermostat chamber at 298 K. The MOTOFIT program was

employed for the reflectivity fitting.[29] SLD values of Si, SiO_2, and D_2O were set to 2.07×10^{-4}, 3.47×10^{-4}, and 6.20×10^{-4} nm^{-2}, respectively. SLD values were calculated employing the NIST neutron scattering calculator. For the PCB, the SLD value was estimated to be 1.29×10^{-4} nm^{-2}, where chemical formula of $C_{10}H_{17}NO_4$ and density of 1.3 g/cm^3 were used for calculation.

2.2.2 Friction Test

Friction tests were conducted employing a homemade ball-on plate type reciprocal tribometer. A high-carbon chromium steel SUJ2 ball probe (diameter 4 mm, Young's modulus 208 GPa, Poisson's ratio 0.30) was placed on the sample fixed on the stage with 0.4 N normal load at room temperature. The average normal pressure P_a was calculated based on the Hertz contact theory to be 406 MPa (see SI). The stage slid over 10 mm at a sliding velocity in the range of 0.2, 0.4, 1.0, or 2.0 cm s^{-1}. The horizontal force was recorded by a load cell. For the friction test under the wet condition, the sliding path area was covered with PBS buffer solution before triggering the friction test. Friction coefficient data were reported as the average of 10 friction tests in the first sliding to obtain averaged data with error bars.

2.3 Preparation of PCB Brush

Silicon substrates were modified with BHE following previous report.[26] CBM (3.54 g, 16.4 mmol) was dissolved in Milli-Q water (4.5 mL). A BHE modified silicon substrate, the CBM solution, methanol (9.0 mL), and a 0.05 M ethyl-2-bromoisobutylate methanol solution (0.82 mL, 0.041 mmol) were introduced in a glass tube, and the solution was degassed by Ar bubbling for 30 minutes. CuBr(I) (15 mg, 0.10 mmol) and 2,2'-bipyridyl (31.6 mg, 0.20 mmol) were dissolved in methanol (1.5 mL) and degassed by three freeze-thaw cycles. A 0.6 mL

portion of the catalyst solution was added into the glass tube, and the glass tube was kept in an oil bath at 30 °C for 16 hours. The PCB brush was washed by shaking in Milli-Q water for 3 hours, then washed thoroughly with running Milli-Q water. The unbound PCB was purified by dialysis, then dried by lyophilization. The number average molecular weight and molecular weight distribution of the unbound PCB were determined by GPC measurement to be 57000 g/mol and 1.79, respectively. The thickness of the dry PCB brushes employed for XPS, contact angle measurement and NR was determined by NR to be 37.3 nm. The graft density of the PCB brush was calculated to be 0.51 chains/nm^2 following previous report.[30]

2.4 Preparation of PCB Brush/BSA Conjugate Film

In a typical run, the PCB brush was soaked in a 0.4 M EDC MES buffer solution (pH 5.0) with or without 0.4 M NHS for 20 minutes at room temperature [Activation Process], then transferred to a 2.5 mg/mL BSA MES buffer solution (pH 5.0) followed by standing for 2 hours at room temperature [Conjugation Process]. The hybrid film was washed with Milli-Q water then stored in a PBS buffer (**Figure 1**).

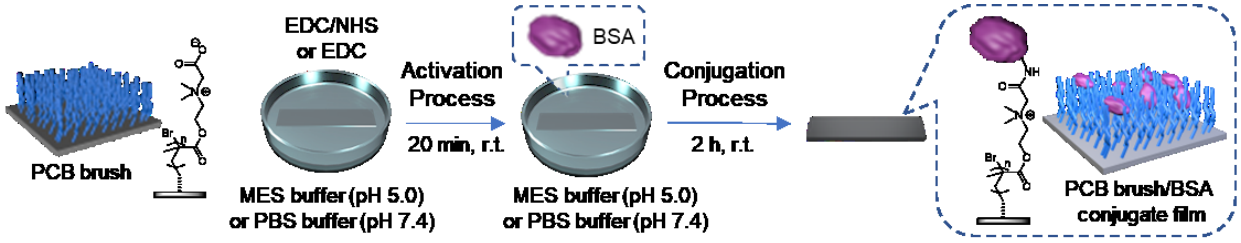

Figure 1. Schematics of PCB brush/BSA conjugation processes

Table 1. Reaction conditions in the PCB brush/BSA conjugation processes

run	Activation Process		Conjugation Process	XPS element compositions			f_{BSA}[a]
	Reagents	Buffer	Buffer	C1s	N1s	O1s	
1	EDC/NHS	MES	MES	66.9	7.58	26.3	0.12
2	EDC/NHS	MES	PBS	65.0	7.01	27.9	0.08
3	EDC/NHS	PBS	MES	65.6	6.89	27.6	0.04
4	EDC/NHS	PBS	PBS	64.9	7.49	27.7	0.04
5	EDC	MES	MES	62.4	14.5	23.2	0.75
6	EDC	MES	PBS	67.2	9.69	23.1	0.43
7	EDC	PBS	MES	66.4	7.37	26.3	0.13
8	EDC	PBS	PBS	65.6	7.40	27.0	0.08

[a]The BSA fractions in the outermost surface were calculated by equation (1).

3. RESULTS AND DISCUSSION

3.1 BSA Conjugation to PCB Brush

We conducted screening of the PCB brush/BSA conjugation process to find the optimum approach to achieve substantial binding of BSA to the PCB brushes. The conjugation processes adopted in this study are summarized in **Table 1**. First, the carboxylate groups in the PCB brush chains were activated by soaking PCB brushes in an EDC buffer solution with or without NHS. This is referred to as the "Activation Process". Second, the PCB brushes were transferred to a BSA buffer solution and allowed to stand for 2 hours at room temperature. This is referred to as the "Conjugation Process". The reagents used and the type of buffer solutions were systematically investigated. The pH of MES and PBS buffer solutions was adjusted to 5.0 and 7.4, respectively.

Figure 2 shows N1s XPS spectra of PCB brushes, BSA films, and PCB brush/BSA conjugate films fabricated through process No. 5 (see **Table 1**), and the XPS survey scan, C1s narrow scan, and O1s narrow scan spectra were shown in **Figure S1**. The C1s, N1s, and O1s element compositions of the PCB brush were approximately consistent with the theoretical values of PCB, and the signals assigned to Si were hardly observed, indicating a thick PCB brush film was prepared without significant defects (**Figure S1**(b)). PCB brushes show an N1s XPS signal assigned to the quaternary ammonium cation groups ($C-N^+$) at 402.3 eV (**Figure 2**(a)), while BSA films show an N1s XPS signal assigned to the amide bonds (C−N) at 399.8 eV (**Figure 2**(b)). Since the PCB brush/BSA conjugate films exhibited the two separated N1s XPS signals, the BSA conjugation efficiency was estimated by the integration ratio of the N1s XPS

signals. The BSA fractions in the outermost surface of the dry conjugate films, f_{BSA}, were calculated by the following equation (1),

$$f_{BSA} = \frac{Integ_{BSA}}{Integ_{PCB}*(13.4/6.83)+Integ_{BSA}} \quad (1)$$

where the $Integ_{PCB}$ and $Integ_{BSA}$ are the integration of the N1s XPS signals obtained by waveform separation, and the factor 13.4/6.83 is the weighting of the N1s composition ratios of BSA and PCB based on the atomic ratio of the N1s normalized by the C1s signal intensity. Interestingly, the process No. 5, where the use of MES buffer without NHS in the activation process and MES buffer in the conjugation process, yielded the most pronounced conjugation of BSA. Other processes, where the use of PBS buffer and/or EDC/NHS combined reagents in the activation process and/or PBS buffer in the conjugation process, resulted in less reaction efficiency (see **Table 1**). To address the cause of process-dependent BSA conjugation yield, the conversion of carboxylate groups in the carboxybetaine units to *O*-acylisourea ester in the activation process was investigated by XPS. The PCB brush after the EDC activation process in the MES buffer and successive wash with water showed a N1s XPS signal assigned to the activated ester at 399.2 eV, while the signal intensity significantly reduced after soaking in the PBS buffer for 2 hours (**Figure S2**). Meanwhile, the PCB brush after the EDC activation process in the PBS buffer and successive wash with water was identical to that of a neat PCB brush. Thus, the carboxylate activation with EDC proceeds in the MES buffer but not in the PBS buffer, and the *O*-acylisourea activated ester is unstable to be hydrolyzed immediately in the PBS buffer.

Thus, the high BSA conjugation efficiency in the acidic MES buffer preferable to neutral PBS buffer is attributed to the high conversion of the activation process. Besides, the isoelectric point of BSA may associate with the BSA conjugation efficiency. BSA is water-soluble, but partially aggregates in water through hydrophobic interaction to produce the dimer and trimer in solution, and may also produce covalently-bonded aggregates via disulfide bonding.[31] The net charge of BSA is neutral at the isoelectric point of 4.7, thereby the BSA molecules tend to aggregate at pH 5.0 due to the loss of electrostatic repulsion. The BSA aggregates are accessible to the activated PCB chains to conjugate efficiently. Meanwhile, in the PBS buffer at pH 7.4, where an appropriate pH for the reaction of carboxylate activated by NHS, the net charge of BSA is negative. The negatively charged BSAs are well-hydrated and repelled from the reaction sites in the vicinity of PCB brushes, thus preventing excessive conjugation to the PCB chains.

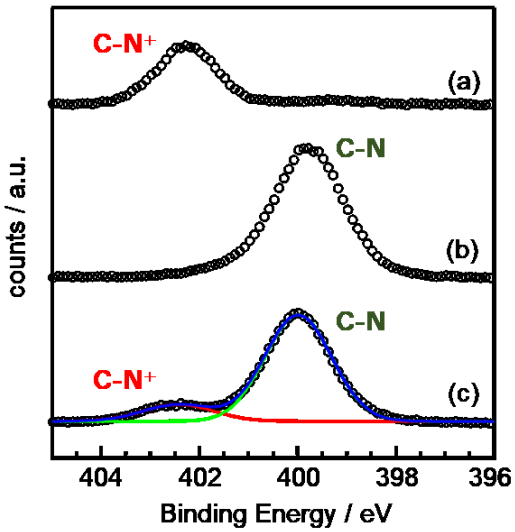

Figure 2. XPS spectra of (a) a PCB brush, (b) a BSA cast film, and (c) a PCB brush/BSA conjugate films fabricated by process No.5 (see **Table 1**). The green and red curves are Gaussian distribution curves with peaks at 402.3 eV and 399.8 eV obtained by waveform separation, and the blue curve is the sum.

Water spread on the PCB brush thin films and showed a low water droplet contact angle (**Figure 3(a)**). As the PCB brushes involve positively charged quaternary ammonium cations and negatively charged carboxylate anions, water show profound interactions with the PCB brush chains. Thus, the interfacial tension between the PCB brush and water is low while the surface tension of the PCB brush is high, leading to the hydrophilic character. Water droplets on the PCB brush/BSA conjugate films fabricated by process No.5 showed a large contact angle of 57 ± 3.7 deg, indicating the BSA conjugation reduces the hydrophilicity of the PCB brush (**Figure 3(b)**). Although BSA is a water-soluble protein, the water affinity is poor in comparison with PCB chains because the BSA includes hydrophobic portions. Meanwhile, the PCB brush/BSA conjugate films repelled hexadecane (HD) droplets in water. The contact angle of a HD droplet was 142 ± 3.2 deg, while the BHE modified silicon wafer showed the HD droplet contact angle of 116 ± 4.2 deg (**Figure S3**). The conjugate films transform immediately by soaking in water to avoid the water contact to the hydrophobic part of BSA because of the activated molecular motion of hydrated PCB and BSA chains. Since the hydrophilic part of the conjugate films is arranged to the water interface, the HD repellency was induced. On the other hand, when HD droplets come into contact, hydrophobic residues in the BSA are segregated to reduce the interfacial energy, then the adhesion energy of the HD increases. The results indicate that the PCB brush/BSA conjugate films exhibit adaptable interfacial properties depending on the interaction with the contact medium due to the amphiphilic nature of BSA and the high molecular mobility of the hydrated PCB and BSA chains.

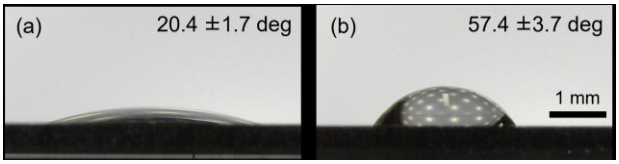

Figure 3. Side view of a water droplet (10 mL) on (a) a PCB brush and (b) a PCB brush/BSA conjugate film fabricated by process No. 5. The averaged contact angle values were shown at the corner of the images.

3.2 Chain Dimension of PCB Brush/BSA Hybrid Thin Films in PBS Buffer

To address the non-uniform structure of the PCB brush/BSA conjugate films produced through the carbodiimide cross-linking reaction, the NR was employed.[32] First, the NR of the PCB brush under dry nitrogen atmosphere was measured. Subsequently, the NR of the identical PCB brush under PCB buffer was measured. Then, the identical PCB brush film was conjugated with BSA through process No. 6, where the BSAs are introduced with the appropriate f_{BSA}, followed by a careful wash with water. The PCB brush/BSA conjugate film was dried in vacuo, then subjected to NR. Finally, the NR of the PCB brush/BSA conjugate film under PCB buffer was measured. It should be noted that the calculated SLD of the PCB is 1.29×10^{-4} nm^{-2}, and that of BSA ranges from approximately 2.4×10^{-4} nm^{-2} to 3.8×10^{-4} nm^{-2} depending on the D_2O fraction of the medium. The NR profiles of the PCB brush and the PCB brush/BSA conjugate film under dry nitrogen gas flow showed a regular oscillation of so-called Kiessig fringe due to the interference of reflected neutrons, indicating the uniform thickness and low interfacial roughness (**Figure 4(A)** upper panel).

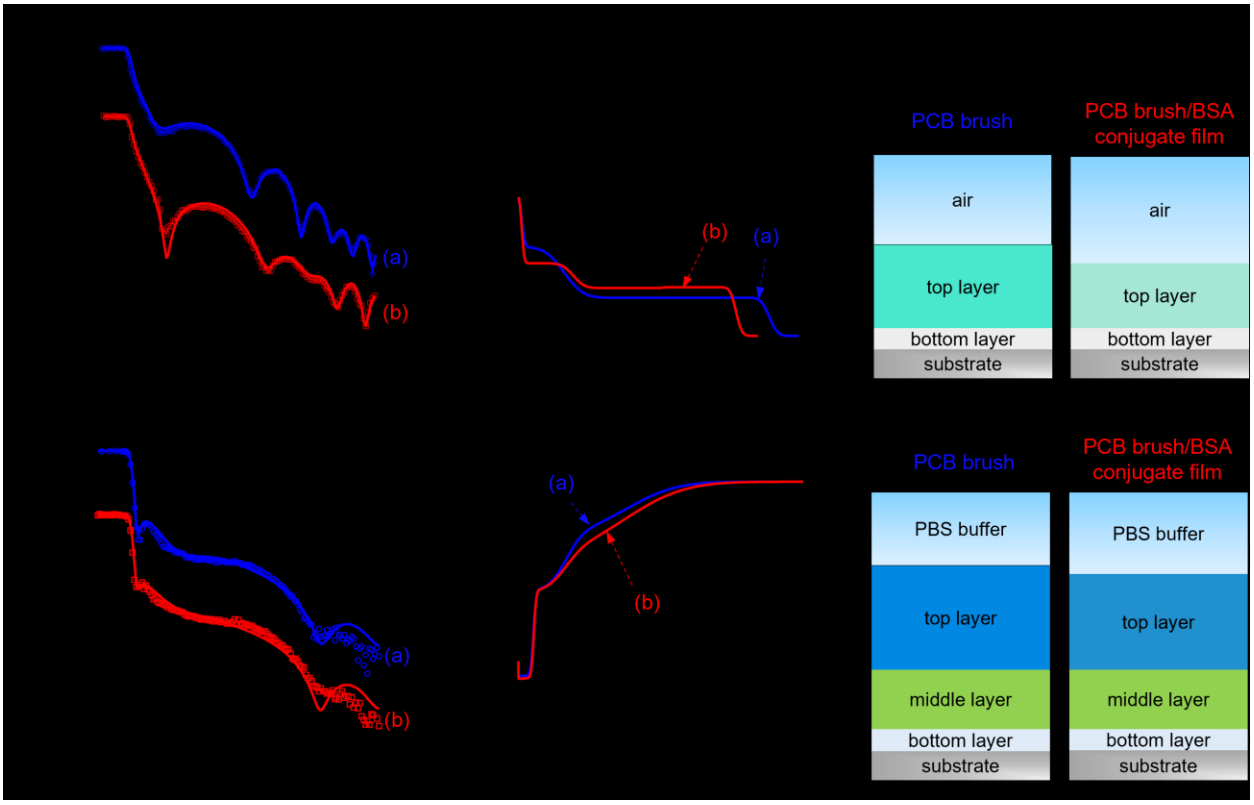

Figure 4. (A) NR profiles (B) SLD profiles, and (C) box layer models of (a) the PCB brush and (b) the PCB brush/BSA conjugate film in (upper panels) dry nitrogen and (lower panels) PBS D_2O buffer at 298 K. The solid lines in NR profiles are fitting curves based on box layer models shown in panel (C). Fitting parameters are shown in **Table S1-4**.

The NR profiles of the PCB brush and PCB brush/BSA conjugate film were reproduced with a distinct two-layer model composed of a thin high SLD bottom layer and a thick low SLD top layer (**Figure 4(B), (C)** upper panel). The fitting parameters are shown in SI. As shown in

the SLD profile, the top layer of the PCB brush exhibited a SLD of 0.93×10^{-4} nm^2 lower than the calculated value of 1.29×10^{-4} nm^{-2}. Although the experiment was performed employing a sealed thermostat sample chamber passing dry nitrogen gas, the hydrophilic PCB brush would retain moisture water whose SLD is -0.56×10^{-4} nm^{-2}. Meanwhile, the PCB brush/BSA conjugate film showed increased SLD of 1.05×10^{-4} nm^2 and thinning. The increase of SLD suggests the conjugation of BSA. Besides, since the relatively hydrophobic BSA molecules are conjugated to the PCB chains, the amount of low SLD water would be reduced leading to the SLD increase and thinning.

The NR profiles of the PCB brush and PCB brush/BSA conjugate film in PBS D_2O buffer are shown in **Figure 4(A)** lower panel. The featureless diffuse NR profiles without significant oscillation indicate increased interfacial roughness and obscured layer boundary. The NR profiles of the PCB brush were reproduced with a distinct three-layer model composed of a thin low SLD bottom layer and a middle layer and a thick high SLD top layer (**Figure 4(B), (C)** lower panel). The PCB brush involves a substantial amount of deuterium oxide as shown in the large SLD of the top layer and the significant interfacial roughness. The middle layer with intermediate SLD is required to fit the reflectivity, indicating the zwitterionic PCB brush consists of distinct nonuniform water content layers. Since the lateral chain density in the swollen PCB brushes increases toward the bottom, the inter-chain interactions and free volume reduction are promoted in the middle layer, thereby the middle layer includes a small amount of water. However, the layer boundary is indistinct in comparison with poly(sulfobetaine) brush, which is a zwitterionic polymer brush previously reported,[20, 33] because of the weak inter-zwitterion interaction of carboxybetaine.[34] Meanwhile, the bottom layer is assigned to the chains that

strongly interact with the solid substrate, and the chains are hardly hydrated as shown in the low SLD identical to the PCB chains.

Both the PCB brush and PCB brush/BSA conjugate film showed a hump at q_z = 0.18-0.20 nm^{-1} that appears immediately after the critical angle of total reflection in the NR profile (**Figure 4(A)** lower panel), while the undulation damping was confirmed in the PCB brush/BSA conjugate film. The variation in NR profiles was reproduced by lowering the SLD of the top layer (**Table S3, S4**). Since the BSA is less swollen to PCB brush chains, the SLD decrease is indicative of BSA conjugation. Interestingly, the SLD variation is only observed in the top layer, while the middle layer is identical to the PCB brush. The top layer thickness was approximately 24.5 nm, which is sufficiently larger than the radius of gyration of BSA (approximately 4 nm in pH 7.4 PBS buffer). Thus, the conjugated BSAs are localized to the top layer, while excluded from the middle layer. This conjugation depth limitation would be attributed to the excluded volume effect and local EDC activation in the activation process. Since the graft density of the PCB brush is 0.51 chains/nm^2, where it could be distinguished as high-density brush while it may be overestimated due to the broad polydispersity of the grafted chains, the bulky BSA molecules cannot penetrate the PCB brush. Besides, since the *O*-acylisourea active ester is bulky, the activation would be limited to the liquid side region. As the result, the BSA conjugation through the EDC cross-linking reaction is limited to the top layer.

The PCB brush/BSA conjugate film showed an almost similar rather thinner swollen thickness to the original PCB brush. The BSA conjugation should result in the thickening of the original PCB brush, but the opposite was the case. BSA is a water-soluble protein, but the hydrophilicity is less than the zwitterionic PCB chain. Thus, the BSA conjugation may deteriorate the hydration of PCB chains in the vicinity of the bound BSA. Besides, the BSA

conjugation may partially crosslink the PCB brush chains because the multiple amines in a BSA may bridge different PCB chains. The networking would result in the swollen thickness reduction of the PCB brush/BSA conjugate film. This argument is supported by the slight SLD reduction of the top layer as shown Figure 4(B) lower panel. The hydration disruption and partial cross-linking are also associated with the thickness reduction in dry nitrogen atmosphere.

3.3 Impact of BSA Conjugation to Tribological Performances of PCB Brush Thin Films

The impact of BSA conjugation on the lubricating performance of zwitterionic PCB brush was verified by a reciprocal friction test (**Figure 5**). PCB brush/BSA conjugate films fabricated through process No. 6, identical to samples applied in NR, were used for the friction test. The coefficients of friction (COF) of the PCB brush in PBS buffer were constant in the sliding velocity range of 0.2 cm/s to 1.0 cm s^{-1}. The friction coefficients were approximately 0.25 with large error bars. In the low sliding velocity range, the sliding mode is so-called boundary lubrication, where the sliding probe and film are so close that the molecular interactions and contact area dominate the friction force.[2] The COFs of PCB brush/BSA conjugate film were lower than PCB brush in the low sliding velocity range. As described above, the conjugated BSAs are localized at the outermost region in the PBS buffer, and the water content reduces by the BSA conjugation. Thus, the BSA conjugation results in the rise of elastic modulus. According to the Amontons-Coulomb law, $F = As$, where F is friction force, A is effective contact area, s: shear strength, the F reduces with decreasing the A. As the effective contact area decreases, the friction force and the COF (= F/w, w: normal load) decrease. On the other hand, the adhesion force associated with the shear strength may be altered by the BSA conjugation,

while the exact value is missing at present. Since the normal pressure is much higher than Young's modulus of hydrated polymer brush and BSA, the electromagnetic interactions between the friction probe and PCB brush/BSA conjugate film become pronounced. The lower friction coefficient of the PCB brush/BSA conjugate film in the low sliding velocity would be also attributed to the electrostatic repulsive interaction of negatively charged BSA and SUSJ2 sliding probe.

Meanwhile, at 2 cm s^{-1} sliding velocity, the COF decreased significantly. The lubrication mode shifted from boundary lubrication to mixed lubrication, where the load is partially supported by the fluid film.[2, 12, 35] In the high sliding velocity region of 2 cm s^{-1}, the COFs of PCB brush/BSA conjugate film was higher than PCB brush. In other words, the BSA conjugation rather deteriorates the lubricity in the mixed lubrication regime. Although the causes for the COF crossover need to be pursued, the water content modulation of the thin films through the BSA conjugation would be coupled with the result. Since the water content in the top layer of the PCB brush thin film reduces by the BSA conjugation, the fluid film promoting effect would be declined in the PCB brush/BSA conjugate film. However, the adhesion force and dynamics of the hydrated chains would also associate with the event, thus requiring further research.

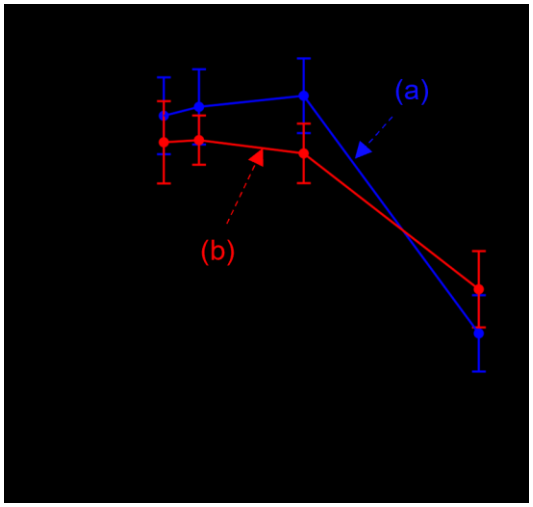

Figure 5. Sliding velocity dependence of the COF of (a) PCB brushes and (b) PCB brush/BSA conjugate films in PBS buffer at 298 K. The error bar is the standard deviation.

CONCLUSION

A facile procedure to conjugate proteins to a zwitterionic PCB brush was developed, and the adaptable wetting performance, nonuniform structure, and lubrication properties of the PCB brush/BSA conjugate films in PBS buffer were addressed. BSA conjugation to a zwitterionic PCB brush was achieved by a carbodiimide crosslinking reaction. The reaction conditions profoundly impact the BSA conjugation efficiency, and the conjugation was most efficient in the acidic MES buffer. The PCB brush/BSA conjugate films exhibit adaptable interfacial properties due to the amphiphilic nature of BSA. The NR showed that the BSAs were localized at the liquid side of the conjugate film, and hardly located inside. The BSA conjugation reduced the water content at the top layer, while the carpet PCB brush layer was well-swollen identical to before conjugation. The PCB brush/BSA conjugate films showed improved lubricity in the boundary

lubrication regime probably due to the decrease in contact area caused by the raise of elastic modulus through BSA conjugation and electrostatic repulsive interactions. This is the first report shedding light to the nonuniform structure of zwitterionic polymer brush/protein conjugate films in buffer solution and coupled the nonuniform swollen structure with the lubrication performance. However, the coefficient of friction was comparable to the conventional single component poly(carboxybetaine) brush. Rational molecular designs including the conjugation of optimum proteins and the synergetic effect with synovial fluids of proteoglycans and glycosaminoglycan are required to achieve further lubrication. This study could be a model system for investigating zwitterion/protein composite interfaces, and valid for the design of biomedical apparatus which require lubrication in vivo.

ASSOCIATED CONTENT

Supporting Information.

The Supporting Information is available free of charge on the ACS Publications website. Measurement conditions, XPS spectra, side view of a hexadecane droplet attached on thin films in Milli-Q water and the contact angle, parameter values for NR profile curve fitting with MOTOFIT (PDF)

AUTHOR INFORMATION

Corresponding Author

Yuji Higaki

Department of Integrated Science and Technology, Faculty of Science and Technology, Oita University, Oita 870-1192, Japan; orcid.org/0000-0002-1032-4661; Email: y-higaki@oita-u.ac.jp

Author Contributions

The manuscript was written through the contributions of all authors. All authors have given approval to the final version of the manuscript. Y.H. conceived and directed the project. R.F. performed the experiments and analyzed the data. T.O. designed the friction test instrument and supported the tribology study. N.L.Y. contributed to the NR experiments.

ACKNOWLEDGMENT

This work was supported by Oita University President's Strategic Discretionary Fund. The NR experiments were performed on the beamline BL16 in the Materials and Life Science Facility (MLF), J-PARC, Japan (program nos. 2019B0108, 2020B0024). The authors acknowledge Y. Saruwatari (Osaka Organic Chemical Industry Ltd.) for the kind donation of the carboxybetaine methacrylate monomer.

ABBREVIATIONS

PCB, poly(carboxybetaine); BSA, bovine serum albumin; NR, neutron reflectivity.

REFERENCES

1. Lee, S.; Spencer, N. D., Sweet, Hairy, Soft, and Slippery. *Science* **2008**, *319*, 575-576.

2. Luengo, G.; Israelachvili, J.; Granick, S., Generalized Effects in Confined Fluids: New Friction Map for Boundary Lubrication. *Wear* **1996**, *200*, 328-335.

3. Lin, W.; Klein, J., Hydration Lubrication in Biomedical Applications: From Cartilage to Hydrogels. *Acc. Mater. Res.* **2022**, *3*, 213-223.

4. Zhao, W.; Zhang, Y.; Zhao, X.; Ji, Z.; Ma, Z.; Gao, X.; Ma, S.; Wang, X.; Zhou, F., Bioinspired Design of a Cartilage-like Lubricated Composite with Mechanical Robustness. *ACS Appl. Mater. Interfaces* **2022**, *14*, 9899-9908.

5. Zhang, X.; Lou, Z.; Yang, X.; Chen, Q.; Chen, K.; Feng, C.; Qi, J.; Luo, Y.; Zhang, D., Fabrication and Characterization of a Multilayer Hydrogel as a Candidate for Artificial Cartilage. *ACS Appl. Polym. Mater.* **2021**, *3*, 5039-5050.

6. Tadmor, R.; Janik, J.; Klein, J.; Fetters, L. J., Sliding Friction with Polymer Brushes. *Phys. Rev. Lett.* **2003**, *91*, 115503.

7. Kobayashi, M.; Terayama, Y.; Hosaka, N.; Kaido, M.; Suzuki, A.; Yamada, N.; Torikai, N.; Ishihara, K.; Takahara, A., Friction Behavior of High-Density Poly(2-methacryloyloxyethyl phosphorylcholine) Brush in Aqueous Media. *Soft Matter* **2007**, *3*, 740-746.

8. Chen, M.; Briscoe, W. H.; Armes, S. P.; Klein, J., Lubrication at Physiological Pressures by Polyzwitterionic Brushes. *Science* **2009**, *323*, 1698-1701.

9. Kobayashi, M.; Takahara, A., Tribological Properties of Hydrophilic Polymer Brushes under Wet Conditions. *Chem. Rec.* **2010**, *10*, 208-216.

10. Chen, M.; Briscoe, W. H.; Armes, S. P.; Cohen, H.; Klein, J., Polyzwitterionic Brushes: Extreme Lubrication by Design. *Eur. Polym. J.* **2011**, *47*, 511-523.

11. Nomura, A.; Okayasu, K.; Ohno, K.; Fukuda, T.; Tsujii, Y., Lubrication Mechanism of Concentrated Polymer Brushes in Solvents: Effect of Solvent Quality and Thereby Swelling State. *Macromolecules* **2011**, *44*, 5013-5019.

12. Kobayashi, M.; Tanaka, H.; Minn, M.; Sugimura, J.; Takahara, A., Interferometry Study of Aqueous Lubrication on the Surface of Polyelectrolyte Brush. *ACS Appl. Mater. Interfaces* **2014**, *6*, 20365-20371.

13. Iuster, N.; Tairy, O.; Driver, M. J.; Armes, S. P.; Klein, J., Cross-Linking Highly Lubricious Phosphocholinated Polymer Brushes: Effect on Surface Interactions and Frictional Behavior. *Macromolecules* **2017**, *50*, 7361-7371.

14. Mandal, J.; Simic, R.; Spencer, N. D., Impact of Dispersity and Hydrogen Bonding on the Lubricity of Poly(acrylamide) Brushes. *Adv. Mater. Interfaces* **2019**, *6*, 1900321.

15. Yan, W.; Romio, S. N. R. M.; Benetti, E. M., Bioinert and Lubricious Surfaces by Macromolecular Design. *Langmuir* **2019**, *35*, 13521-13535.

16. Trachsel, L.; Ramakrishna, S. N.; Romio, M.; Spencer, N. D.; Benetti, E. M., Topology and Molecular Architecture of Polyelectrolytes Determine Their pH-Responsiveness When Assembled on Surfaces. *ACS Macro Lett.* **2021**, *10*, 90-97.

17. Paschke, S.; Lienkamp, K., Polyzwitterions: From Surface Properties and Bioactivity Profiles to Biomedical Applications. *ACS Appl. Polym. Mater.* **2020**, *2*, 129-151.

18. Ishihara, K., Blood-Compatible Surfaces with Phosphorylcholine-Based Polymers for Cardiovascular Medical Devices. *Langmuir* **2019**, *35*, 1778-1787.

19. André Laschewsky, A. R., Molecular Design of Zwitterionic Polymer Interfaces: Searching for the Difference. *Langmuir* **2019**, *35*, 1056-1071.

20. Higaki, Y.; Kobayashi, M.; Takahara, A., Hydration State Variation of Polyzwitterion Brushes through Interplay with Ions. *Langmuir* **2020**, *36*, 9015-9024.

21. Baggerman, J.; Smulders, M. M. J.; Zuilhof, H., Romantic Surfaces: A Systematic Overview of Stable, Biospecific, and Antifouling Zwitterionic Surfaces. *Langmuir* **2019**, *35*, 1072-1084.

22. Badoux, M.; Billing, M.; Klok, H.-A., Polymer Brush Interfaces for Protein Biosensing Prepared by Surface-Initiated Controlled Radical Polymerization. *Polym. Chem.* **2019**, *10*, 2925-2951.

23. Weltz, J. S.; Kienle, D. F.; Schwartz, D. K.; Kaar, J. L., Dramatic Increase in Catalytic Performance of Immobilized Lipases by Their Stabilization on Polymer Brush Supports. *ACS Catal.* **2019**, *9*, 4992-5001.

24. Sweryda-Krawiec, B.; Devaraj, H.; Jacob, G.; Hickman, J. J., A New Interpretation of Serum Albumin Surface Passivation. *Langmuir* **2004**, *20*, 2054-2056.

25. Nakashima, K.; Sawae, Y.; Murakami, T., Study on Wear Reduction Mechanisms of Artificial Cartilage by Synergistic Protein Boundary Film Formation. *JSME Int. J.* **2005**, *48*, 555-561.

26. Ohno, K.; Morinaga, T.; Koh, K.; Tsujii, Y.; Fukuda, T., Synthesis of Monodisperse Silica Particles Coated with Well-Defined, High-Density Polymer Brushes by Surface-Initiated Atom Transfer Radical Polymerization. *Macromolecules* **2005**, *38*, 2137-2142.

27. Mitamura, K.; Yamada, N. L.; Sagehashi, H.; Torikai, N.; Arita, H.; Terada, M.; Kobayashi, M.; Sato, S.; Seto, H.; Goko, S.; Furusaka, M.; Oda, T.; Hino, M.; Jinnai, H.; Takahara, A., Novel Neutron Reflectometer SOFIA at J-PARC/MLF for In-Situ Soft-Interface Characterization. *Polym. J.* **2013**, *45*, 100-108.

28. Yamada, N. L.; Torikai, N.; Mitamura, K.; Sagehashi, H.; Sato, S.; Seto, H.; Sugita, T.; Goko, S.; Furusaka, M.; Oda, T.; Hino, M.; Fujiwara, T.; Takahashi, H.; Takahara, A., Design and Performance of Horizontal-Type Reutron Reflectometer SOFIA at J-PARC/MLF. *Eur. Phys. J. Plus* **2011**, *126*, 108.

29. Nelson, A., Co-Refinement of Multiple-Contrast Neutron/X-ray Reflectivity Data Using MOTOFIT. *J. Appl. Crystallogr.* **2006**, *39*, 273-276.

30. Husseman, M.; Malmström, E. E.; McNamara, M.; Mate, M.; Mecerreyes, D.; Benoit, D. G.; Hedrick, J. L.; Mansky, P.; Huang, E.; Russell, T. P., Controlled Synthesis of Polymer Brushes by "Living" Free Radical Polymerization Techniques. *Macromolecules* **1999,** *32*, 1424-1431.

31. Jordan, G. M.; Yoshioka, S.; Terao, T., The Aggregation of Bovine Serum Albumin in Solution and in the Solid State. *J. Pharm. Pharmacol.* **1994**, *46*, 182-185.

32. Delcea, M.; Helm, C. A., X-ray and Neutron Reflectometry of Thin Films at Liquid Interfaces. *Langmuir* **2019**, *35*, 8519-8530.

33. Sakamaki, T.; Inutsuka, Y.; Igata, K.; Higaki, K.; Yamada, N. L.; Higaki, Y.; Takahara, A., Ion-Specific Hydration States of Zwitterionic Poly(sulfobetaine methacrylate) Brushes in Aqueous Solutions. *Langmuir* **2018**, *35*, 1583-1589.

34. Shao, Q.; Jiang, S., Molecular Understanding and Design of Zwitterionic Materials. *Adv. Mater.* **2014**, *27*, 15-26.

35. Igata, K.; Sakamaki, T.; Inutsuka, Y.; Higaki, Y.; Okajima, M. K.; Yamada, N. L.; Kaneko, T.; Takahara, A., Cationic Polymer Brush/Giant Polysaccharide Sacran Assembly: Structure and Lubricity. *Langmuir* **2020**, *36*, 6494-6501.

TOC Graphics